# Rodeo Algorithm with Controlled Reversal Gates

Max Bee-Lindgren,<sup>1</sup> Zhengrong Qian,<sup>2</sup> Matthew DeCross,<sup>3</sup> Natalie C. Brown,<sup>3</sup> Christopher N. Gilbreth,<sup>3</sup> Jacob Watkins,<sup>2</sup> Xilin Zhang,<sup>2</sup> and Dean Lee<sup>2</sup>

<sup>1</sup>School of Physics, Georgia Institute of Technology, Atlanta, GA 30332, USA
<sup>2</sup>Facility for Rare Isotope Beams and Department of Physics and Astronomy, Michigan State University, MI 48824, USA
<sup>3</sup>Quantinuum, 303 S. Technology Ct., Broomfield, Colorado 80021, USA

Many quantum algorithms use a process called controlled time evolution, where the system of interest evolves in time only if an auxiliary (or ancilla) qubit is in a particular state. We show that this process can be implemented efficiently using controlled reversal gates. A reversal gate R is a product of single qubit gates that anticommutes with some subset of terms in the quantum Hamiltonian, and the controlled reversal gate  $C_R$  is the implementation of R controlled by the ancilla qubit. By flipping the sign of terms in the Hamiltonian, the flow of time is toggled forwards and backwards depending on the state of the ancilla. In this work, we use controlled reversal gates and the rodeo algorithm to compute the energy spectrum of a two-qubit Hamiltonian; the use of controlled reversal gates provides a five-fold reduction in the number of two-qubit entangling gates needed for the example considered here. We use the Quantinuum H1-2 and IBM Perth devices to realize the quantum circuits. While the Quantinuum H1-2 achieves a significantly lower error rate than the IBM Perth, we were able to determine the energy levels on both devices with an error of less than 0.06% of the full span of the energy spectrum when using five cycles of the rodeo algorithm. We also discuss the expected performance for larger quantum systems, and we find that the reduction factor in the number of gates is even greater for larger, multi-qubit systems.

#### INTRODUCTION

Quantum computing offers the potential for efficient eigenvalue estimation and eigenstate preparation for quantum many body systems. There are several well-known algorithms that measure energy eigenvalues by means of time evolution controlled by an auxiliary register of qubits. Some examples include quantum phase estimation [1–3] iterative quantum phase estimation [4, 5]. The rodeo algorithm (RA) is another recently introduced method that uses time evolution controlled by an auxiliary register of qubits [6]. It is a stochastic algorithm that uses destructive interference to suppress eigenvectors with eigenvalues different from the desired target energy. It was shown to be exponentially faster than quantum phase estimation and adiabatic evolution [7, 8] for preparing eigenstates [6].

The first implementation of the rodeo algorithm was performed in Ref. [9] for a single qubit Hamiltonian. However the use of controlled time evolution makes the implementation for a multi-qubit system significantly more difficult. In this work, we show that this process can be implemented conveniently using *controlled reversal gates*. In the following, we explain what a controlled gate is and how it is implemented for our two-qubit Hamiltonian. We then perform the rodeo algorithm for the two-qubit Hamiltonian on Quantinuum H1-2 and IBM Perth quantum devices. We present the methods and results and then discuss the performance and prospects for addressing larger quantum systems.

## IMPLEMENTATION FOR A TWO-QUBIT SYSTEM

In this work we consider the two-qubit Hamiltonian

$$H_{\text{obj}} = c_1 X_1 \otimes Z_2 + c_2 Z_1 \otimes X_2 \tag{1}$$

where X and Z are the Pauli operators on the corresponding qubits 1 and 2. Following the notation of Ref. [6, 9], we call this the object Hamiltonian. We take the coefficients to be  $c_1=2.5$  and  $c_2=1.5$ , and the Hamiltonian has eigenvalues at  $\pm c_1 \pm c_2$ . The quantum circuit implementation for the time evolution of the Hamiltonian is shown in Fig. 1. The structure of the Hamiltonian  $H_{\rm obj}$  is chosen so that the time evolution can be performed with only two two-qubit entangling gates, rather than the general case with three two-qubit entangling gates [10, 11]. This feature allows us to perform the rodeo algorithm with less accumulation of gate errors. While the effect of gate errors on the Quantinuum H1-2 machine is not a major concern for the system we consider, it does become a significant issue for the IBM Perth device.

Each cycle of the rodeo algorithm uses a controlled time evolution with a random time t sampled from a normal distribution with zero mean and standard deviation  $\sigma$ . For any given rodeo cycle, the measurement of  $|0\rangle$  for the ancilla corresponds to a successful measurement. Let  $|\psi_I\rangle$  be the initial state and let  $|E_k\rangle$  denote the energy eigenstates of  $H_{\rm obj}$  with energy  $E_k$ . If we apply n cycles of the rodeo algorithm and average over many random trials, the probability of success for all n cycles at energy E is

$$P_n(E) = \sum_{k} \frac{\left[1 + e^{-(E_k - E)^2 \sigma^2 / 2}\right]^n |\langle E_k | \psi_I \rangle|^2}{2^n}.$$
 (2)

We see that there are peaks centered at each energy eigenvalue  $E_k$  where the initial state has nonzero overlap with  $|E_k\rangle$ . We also see that there is a constant background value of  $\frac{1}{2^n}$  for values of E that are significantly further than  $\sigma^{-1}$  away from all energy eigenvalues.

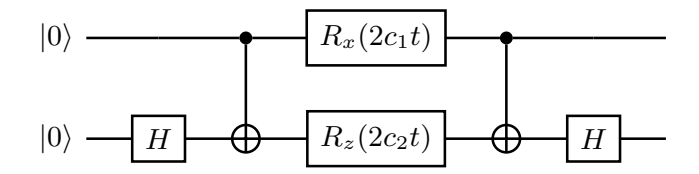


FIG. 1. The quantum circuit for the time evolution of the two-qubit system used for our implementation of the rodeo algorithm.

## CONTROLLED REVERSAL GATES

The suppression of eigenstates with energy  $E_{\rm obj} \neq E$  in Eq. (2) is the result of destructive interference generated by the controlled time evolution. Traditionally, we have time evolution when the ancilla qubit is in state  $|1\rangle$  and no time evolution for state  $|0\rangle$ . For systems with more than one qubit, implementing the controlled time evolution in this manner significantly increases the circuit gate depth. When implemented using the IBM Qiskit transpiler [12] under the assumption of full connectivity between all qubits, directly controlling the time evolution of the circuit in Fig. 1 with an ancilla qubit requires a total of 20 CNOT gates. For the Quantinuum H1-2 device, the two-qubit entangling gate is the  $R_{ZZ}$  gate with angle  $\pi/2$ , and one needs 20  $R_{ZZ}$  gates for the analogous circuit. With only partial connectivity, the number of entangling two-qubit gates grows even larger. For three cycles of the rodeo algorithm, we need 60 two-qubit gates. For five cycles of the rodeo algorithm, we need 100 two-qubit gates. For systems with more than two qubits, the problem is even more severe since the number of two-qubit gates will also scale with the number of Trotter-Suzuki time steps.

Fortunately, the number of two-qubit entangling gates required can be reduced very significantly by using controlled reversal gates. A reversal gate R is a product of single qubit gates  $R = G_1G_2\cdots G_N$  that anticommutes with some subset of terms in the quantum Hamiltonian,  $H_1+\cdots H_M$ . If the Hamiltonian is written as a sum of products of Pauli gates, then it is straightforward to partition the terms in the Hamiltonian so that each partition has some corresponding reversal gate. A controlled reversal gate  $C_R$  is the controlled version of R. In other words,  $C_R = C_{G_1}C_{G_2}\cdots C_{G_N}$ , where each gate is controlled by the  $|0\rangle$  state of a single ancilla qubit. This allows one to toggle the flow of time forwards and backwards, depending on the state of the ancilla.

We use the fact that the relative phase between the states entangled with the ancilla states  $|0\rangle$  and  $|1\rangle$  is relevant for quantum interference while any overall phase factor multiplying both states is irrelevant. It is important that the forward time evolution operator U(t) and the backward time evolution operator U(-t) are inverses of each other. For our two-qubit Hamiltonian example, this reversal-inverse condition is trivially satisfied. We have  $U(t) = e^{-iH_{\rm obj}t}$  and therefore  $U(-t) = e^{iH_{\rm obj}t} = [U(t)]^{-1}$ . For multi-qubit Hamiltonians, the reversal-inverse condition is satisfied if the time evolution operator for one Trotter-Suzuki time step is cho-

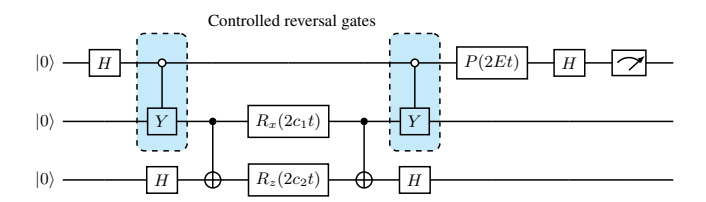


FIG. 2. Circuit diagram for one cycle of the rodeo algorithm on the two-qubit system. The ancilla is shown on top, and the controlled reversal gates are the pair of  $C_Y$  gates. The phase gate P(2Et) multiplies a phase of  $\exp(i2Et)$  to the  $|1\rangle$  state of the ancilla and cancels the relative phase produced by the controlled time evolution for an eigenstate with energy E.

sen so that  $U(-dt) = [U(dt)]^{-1}$ . This is automatically satisfied by the standard Trotter-Suzuki formula at second order [13, 14]. Since the controlled reversal gates implement forward or backward time evolution depending on the ancilla state, the relative phase between the two states evolves at twice the rate and we can reduce the number of Trotter-Suzuki time steps by a factor of two. This feature provides a significant performance advantage for noisy quantum devices.

#### IDENTIFYING ENERGY EIGENVALUES

We now use controlled reversal gates and the rodeo algorithm to compute the energy spectrum of our two-qubit object Hamiltonian. We note that the Pauli operators  $Y_1$  and  $Y_2$  both anticommute with  $H_{\rm obj}$ . We choose  $C_{Y_1}$  for our controlled reversal gate. One cycle of the rodeo algorithm for our system is shown in Fig. 2. It consists of a pair of controlled reversal gates controlled by a single ancilla qubit followed by mid-circuit measurement. By implementing the controlled reversal gates, we are able to reduce the number of two-qubit entangling gates required for each rodeo cycle from 20 to 4.

Our search for the energy eigenvalues consists of three separate scans. Each subsequent scan has a finer resolution and smaller range. The energy range for the first scan is chosen to be from -5 to 5. These values are determined using the Gershgorin circle theorem [15] together with some extra padding to allow for the tails of the probability distribution. The purpose of our coarse-grained first scan ( $\sigma = 4$ ) is to locate all possible regions of the energy spectrum with energy eigenvalue peaks. We identify any region with a success probability well above the average background value of  $\frac{1}{2^n}$  as a candidate for the more focused second scan with finer resolution ( $\sigma = 14$ ). Later in our discussion we give the expected statistical error  $\epsilon_n(E)$  associated with our measurement of  $P_n(E)$ . The second scan is used to more finely determine the structure of the peaks associated with each energy eigenvalue. The third and final scan uses the finest resolution ( $\sigma = 24$ ) in order to accurately determine the center of each eigenvalue peak. The final scan consists of about twenty circuits spanning a narrow region around each peak identified in the second scan.

## IBM AND QUANTINUUM RESULTS

We performed the rodeo algorithm using three cycles and five cycles on the IBM Perth machine. We also performed the rodeo algorithm using five cycles on the Quantinuum H1-2 machine. The success probability versus energy for three cycles on IBM Perth is shown in Fig. 3, starting from the initial state  $|\psi_I\rangle=|00\rangle$ . As described above, the first scan is perform with  $\sigma=4$ , the second scan with  $\sigma=14$ , and third and final scan with  $\sigma=24$ . The curve with the dashed lines shows the exact analytical results given by Eq. (2) for  $\sigma=4$ . We also show the results for the first scan using a noiseless classical simulation.

Let  $N_c$  be the number of distinct circuits implemented in a given scan, each with a unique set of Gaussian random values for the times. Let  $N_s$  be the number of shots used for each circuit. The observed success probability  $P_n(E)$  for n cycles equals the number of successful measurements of 0's for all n cycles divided by  $N_sN_c$ . For all the circuits performed in this study, we use  $N_s=1024$ . For the first scan we take  $N_c=5$ , for the second scan  $N_c=2$ , and for the final scan  $N_c=1$ . Since we are drawing from a binomial distribution, we can estimate that the one-standard-deviation statistical error for our measurement of  $P_n(E)$  will be  $\epsilon_n(E)=\sqrt{P_n(E)[1-P_n(E)]/(N_sN_c)}$ . Since the success probability has a peak at each energy eigenvalue,  $E_k$ , we can fit a Gaussian function to each peak in the final scan data and determine the eigenvalues  $E_k$ .

The results of the fit for three cycles on IBM Perth are shown in the third column of Table I. For this case, the peak success probabilities for the first scan are about 15% lower than the values from the noiseless classical simulations. The average CNOT error for the portion of the IBM Perth device used is about 1%, and we expect that the largest source of noise is due to the 12 CNOT gates needed for each circuit. When compared with the exact results, the RMS deviation for the four eigenvalues is 0.010, which is 0.12% of the full range of the energy spectrum. Meanwhile, the RMS value for the one-sigma uncertainties of the four eigenvalues is 0.006 or 0.07% of the full energy range. We observe that the relative accuracy of the energy measurement is far better than the fidelity of the quantum circuits and is a striking example of the strong noise resilience of the rodeo algorithm.

The success probability versus energy for five cycles on IBM Perth are shown in Fig. 4. In this case we see that the peak success probabilities for the first scan are about 30% lower than the values from the noiseless classical simulations — a significant reduction in performance. In this case we are using 20 CNOT gates. The results of the fit for five cycles on IBM Perth are shown in the fourth column of Table I. When compared with the exact results, the RMS deviation for the four eigenvalues is 0.004, which is 0.05% of the full range of the energy spectrum. The RMS value for the one-sigma uncertainties of the four eigenvalues is 0.003 or 0.04% of the full energy range. We observe that the relative accuracy of the

energy measurement is many orders of magnitude better than the roughly 30% error rate for the quantum circuits.

The success probability versus energy for five cycles on the Quantinuum H1-2 are shown in Fig. 5, starting from the same initial state  $|\psi_I\rangle = |00\rangle$ . In strong contrast with the IBM Perth results, the peak success probabilities for the first scan are close to those from the noiseless classical simulations, as one might expect due to the much better gate fidelities for the Quantinuum H1-2. The error rate for the  $R_{ZZ}$  gate is 0.3%, and the error rate for the  $20~R_{ZZ}$  gates needed for five cycles explains the approximately 5\% reduction in peak heights compared with noiseless simulations. The results of the fit for five cycles on the Quantinuum H1-2 are shown in the fifth column of Table I. When compared with the exact results, the RMS deviation for the four eigenvalues is 0.005, which is 0.06\% of the full range of the energy spectrum. The RMS value for the one-sigma uncertainties of the four eigenvalues is 0.003 or 0.03% of the full energy range. We again see that the accuracy of the energy measurement is several orders of magnitude better than the roughly 5% error rate for the quantum circuits.

The noise robustness of the rodeo algorithm comes from the fact that it implements a simple strategy of reducing the spectral weight of eigenstates with the wrong energy [9]. While noise will reduce the spectral weight of the desired eigenstate, the associated eigenvalue peak will still be visible if the peak height is not reduced below the random background level. Therefore, we expect the peak height to be reduced by noise, but the peak location should be unaffected. This is clearly demonstrated in the results described above.

As a simple model, one can suppose a noisy implementation of the Hamiltonian effectively shifts the kth energy eigenvalue by a random, normally-distributed amount  $\delta E_k$ , which may be correlated or uncorrelated among cycles. Inserting  $\delta E_k$  into Eq. (2) and averaging over the noise shows that this will reduce the height and increase the width of the peak in  $P_n(E)$  corresponding to  $E_k$ , but leave the peak center, and hence the measured energy eigenvalue, unchanged (see the Supplemental Material for further details).

## DISCUSSION AND OUTLOOK

We have used controlled reversal gates and the rodeo algorithm to compute the energy spectrum of a two-qubit Hamiltonian. While the Quantinuum H1-2 achieves a significantly lower error rate than the IBM Perth, we were able to determine the energy levels on both devices with an error of less than 0.06% of the full span of the energy spectrum when using five cycles. In order to determine energy eigenvalues accurately, the rodeo algorithm needs only to be able to distinguish the peak associated with an energy eigenvalue above the background level of  $\frac{1}{2^n}$ . Once this threshold criterion is reached, the accuracy of the rodeo algorithm for determining energy eigenvalue is set by the sharpness of the energy eigenvalue peaks in Eq. (2). The width of the peak scales as  $(\sqrt{n}\sigma)^{-1}$ , where n is the number of cycles and  $\sigma$  is the

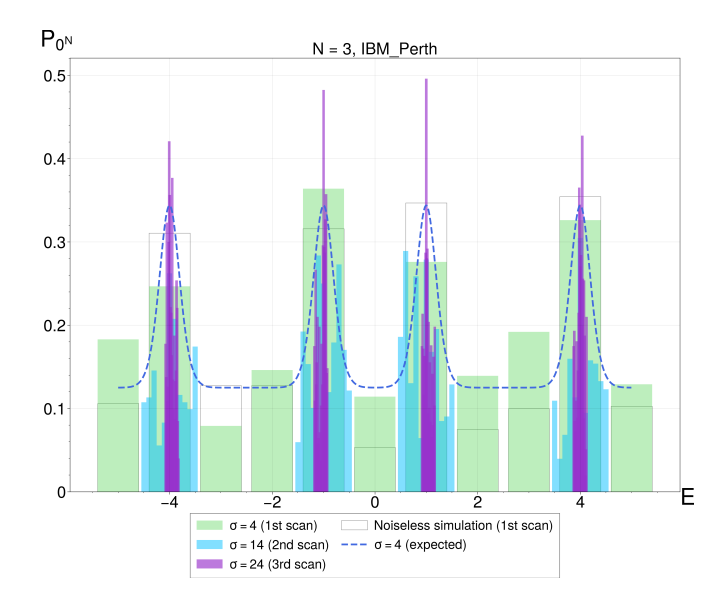


FIG. 3. Results obtained using the ibm\_perth system with three cycles. Compared to the five-cycle run on ibm\_perth, there is more background noise  $(\frac{1}{8} \text{ versus } \frac{1}{32})$  but the success probability is much closer to the values from the noiseless simulation.

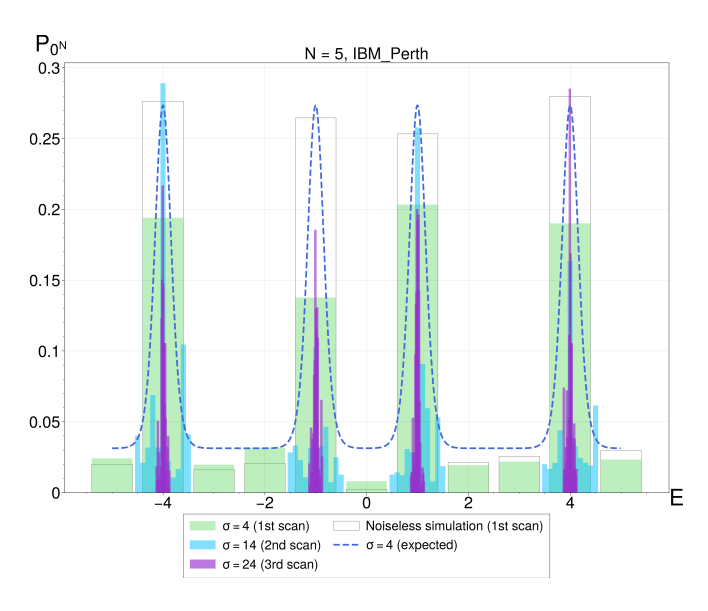


FIG. 4. Results obtained using the ibm\_perth system with five cycles. Again, the dashed line shows the classically calculated success probability. Compared to the run on Quantinuum H1-2, the success probability from the quantum device is significantly lower than that of the noiseless simulation.

standard deviation of the Gaussian random times. We have demonstrated here that with n=3 cycles of the rodeo algorithm and  $\sigma=24$ , we can resolve the energy eigenvalue with an error of about 0.010 on IBM Perth, or  $0.42(\sqrt{n}\sigma)^{-1}$ . With n=5 cycles of the rodeo algorithm and  $\sigma=24$ , we can resolve the energy eigenvalue with an error of about 0.005 on IBM Perth, or  $0.27(\sqrt{n}\sigma)^{-1}$ ; on Quantinuum H1-2, we can resolve the energy eigenvalue with an error of about 0.006, or  $0.32(\sqrt{n}\sigma)^{-1}$ .

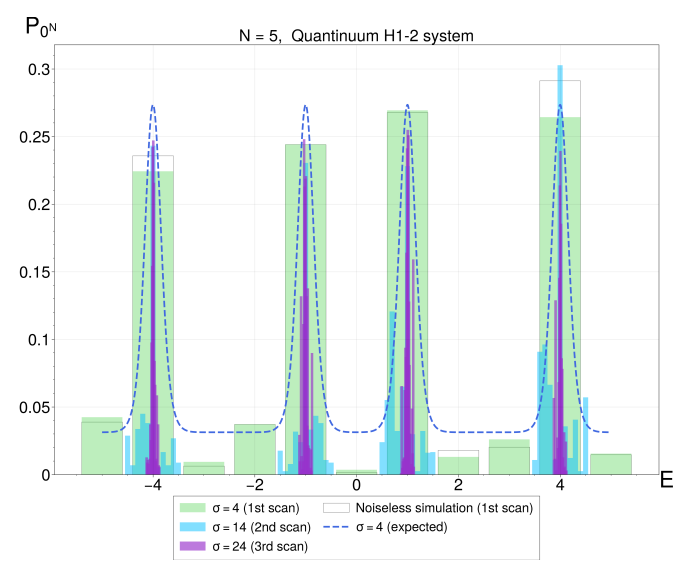


FIG. 5. Results obtained using the Quantinuum H1-2 system with five cycles. The dashed line indicates the expected success probability from classical calculations for the first pass, and the white boxes are the noiseless simulations at the energies of first pass.

We now consider the performance of the rodeo algorithm for the generalization of our Hamiltonian to a one-dimensional chain with N qubits,

$$H_{\text{obj}} = \sum_{n=0}^{N-1} (c_1 X_n \otimes Z_{n+1} + c_2 Z_n \otimes X_{n+1}).$$
 (3)

For notational convenience we assume that N is even. We perform the time evolution using the second-order Trotter-Suzuki approximation with time step dt [13, 14]. This involves alternating the time evolution of the even-n and odd-n terms in Eq. (3). If the N-qubit system is evolved for time duration  $\sigma$ , then the total number of two-qubit exponentials required is  $N\sigma/dt + N/2$ . If the controlled time evolution is implemented in a straightforward manner [12], the number of two-qubit entangling gates is  $20N\sigma/dt + 10N$ . If instead we use the controlled reversal gate  $\prod_{n \text{ even}} C_{Y_n}$ , where the product of controlled-Y gates is over all even qubits, then only  $N\sigma/dt + 2N$  two-qubit entangling gates are required. This is a roughly twenty-fold reduction in the number of gates. If we use the values  $\sigma = 6$  and dt = 0.2, we arrive at 32N twoqubit entangling gates per rodeo cycle. In order for the peak probability to rise above the background value of  $\frac{1}{2^n}$ , the error rate per two-qubit entangling gate should be less than about  $\frac{1}{64N}$ . For an error rate of 0.3% we get  $N \leq 5$ , and for an error rate of 0.1% we get  $N \leq 16$ . Without controlled reversal gates, the corresponding values of N are reduced by a factor of twenty. This shows quite clearly the utility of the controlled reversal gates. We should mention that larger values of N are possible if high statistics with many Gaussian random times are used to make the background signal a smooth function of energy so that smaller peaks are also visible.

In addition to these constraints, we also need that the over-

lap between the initial state and eigenstate of interest is not much smaller than 1. One simple way to increase the initial state overlap is by using quantum adiabatic evolution as a preconditioner. This technique is discussed in Ref. [6]. Other preconditioning techniques based on renormalization group methods are also under current investigation. The estimates we have discussed here give an estimate of what should be possible using the rodeo algorithm and controlled reversal gates in the near future.

Before concluding, we should note that controlled reversal gates also have interesting and useful applications that go well beyond the scope of this work. Work is currently in progress to use controlled reversal gates to efficiently implement fermion antisymmetrization for quantum many-body simulations. Another potential application of controlled reversal gates is the efficient implementation of quantum phase estimation [1, 2, 4, 5] and as well as other state preparation algorithms using controlled time evolution [3, 16].

|  |                  | Exact   | IBM Perth    | IBM Perth   | Quantinuum H1-2 |
|--|------------------|---------|--------------|-------------|-----------------|
|  |                  |         | Three Cycles | Five Cycles | Five Cycles     |
|  | $ \psi_0\rangle$ | -4.0000 | -4.0022(49)  | -4.0006(42) | -3.9982(21)     |
|  | $ \psi_1\rangle$ | -1.0000 | -0.9829(56)  | -0.9927(40) | -1.0083(39)     |
|  | $ \psi_2\rangle$ | 1.0000  | 1.0007(26)   | 1.0008(19)  | 1.0028(22)      |
|  | $ \psi_3\rangle$ | 4.0000  | 4.0093(84)   | 3.9982(25)  | 4.0036(17)      |

TABLE I. Energy eigenvalue estimates from the final pass of the rodeo algorithm with differing numbers of cycles on different devices. The exact values are provided for comparison.

Acknowledgements We are grateful for discussions with Joey Bonitati, Eli Chertkov, Michael Foss-Feig, Gabriel Given, David Hayes, Caleb Hicks, Brian Neyenhuis, Danny Samuel, and Jacob Watkins. We also thank Jay Gambetta and IBM Q for the research accounts and access to hardware. We acknowledge financial support from the U.S. Department of Energy (DE-SC0021152 and DE-SC0013365) and the NU-CLEI SciDAC-4 collaboration.

- [1] D. S. Abrams and S. Lloyd, Phys. Rev. Lett. 83, 5162 (1999), quant-ph/9807070. 1, 5
- [2] R. Cleve, A. Ekert, C. Macchiavello, and M. Mosca, Proceedings of the Royal Society of London Series A 454, 339 (1998), quant-ph/9708016. 5
- [3] P. Siwach and D. Lacroix, Phys. Rev. A 104, 062435 (2021), 2106.10867. 1, 5
- [4] A. Yu. Kitaev, Electronic Colloquium on Computational Complexity 3 (1995), quant-ph/9511026. 1, 5
- [5] K. M. Svore, M. B. Hastings, and M. Freedman, Quant. Inf. Comp. 14, 306 (2013), 1304.0741. 1, 5
- [6] K. Choi, D. Lee, J. Bonitati, Z. Qian, and J. Watkins, Phys. Rev. Lett. 127, 040505 (2021), 2009.04092. 1, 5
- [7] E. Farhi, J. Goldstone, S. Gutmann, and M. Sipser (2000), quant-ph/0001106. 1

- [8] N. Wiebe and N. S. Babcock, New Journal of Physics 14, 013024 (2012). 1
- [9] Z. Qian, J. Watkins, G. Given, J. Bonitati, K. Choi, and D. Lee (2021), 2110.07747. 1, 3
- [10] F. Vatan and C. Williams, Phys. Rev. A 69, 032315 (2004), quant-ph/0308006. 1
- [11] A. Smith, M. S. Kim, F. Pollmann, and J. Knolle, npj Quantum Information 5, 106 (2019), ISSN 2056-6387, URL https:// doi.org/10.1038/s41534-019-0217-0. 1
- [12] M. S. Anis, Abby-Mitchell, H. Abraham, AduOffei, R. Agarwal, G. Agliardi, M. Aharoni, V. Ajith, I. Y. Akhalwaya, G. Aleksandrowicz, et al., *Qiskit: An open-source framework for quantum computing* (2021). 2, 4
- [13] M. Suzuki, Proceedings of the Japan Academy, Series B 69, 161 (1993). 2, 4
- [14] N. Hatano and M. Suzuki, in *Lecture Notes in Physics, Berlin Springer Verlag*, edited by A. Das and B. K. Chakrabarti (2005), vol. 679, p. 37. 2, 4
- [15] S. A. Gershgorin, Bull. Acad. Sci. URSS 1931, 749 (1931). 2
- [16] A. Roggero, C. Gu, A. Baroni, and T. Papenbrock, Phys. Rev. C 102, 064624 (2020), 2009.13485.

## SUPPLEMENTAL MATERIALS

## Success probabilities

For each rodeo cycle, the random times t are selected according to the normalized Gaussian distribution

$$p(t) = \frac{1}{\sqrt{2\pi}\sigma}e^{-\frac{t^2}{2\sigma^2}}.$$
(4)

If our initial is an eigenstate with energy  $E_k$ , then the success probability for one cycle with target energy E is

$$\frac{1}{\sqrt{2\pi}\sigma} \int dt e^{-\frac{t^2}{2\sigma^2}} \cos^2[(E_k - E)\frac{t}{2}] = \frac{1 + e^{-(E_k - E)^2\sigma^2/2}}{2},\tag{5}$$

and the probability of success for all n cycles is

$$\left[\frac{1 + e^{-(E_k - E)^2 \sigma^2 / 2}}{2}\right]^n. \tag{6}$$

Let us now consider an initial state  $|\psi_I\rangle$ , which we can decompose into energy eigenstates

$$|\psi_I\rangle = \sum_k \langle E_k | \psi_I \rangle | E_k \rangle. \tag{7}$$

With this initial state, the success probability after n rodeo cycles will then equal

$$P_n(E) = \sum_{k} \frac{\left[1 + e^{-(E_k - E)^2 \sigma^2 / 2}\right]^n |\langle E_k | \psi_I \rangle|^2}{2^n}.$$
 (8)

## Noisy Hamiltonian evolution

Consider a simple noise model in which the circuit still implements Hamiltonian time evolution for each cycle, but noise in the Hamiltonian shifts the energy eigenvalues  $E_k$  by some amount  $\delta E_{k,i}$  for the *i*th cycle of the algorithm, where  $\delta E_{k,i}$  is random shot-to-shot and is independently distributed between cycles. To first order in the noise, the eigenvectors  $|E_k\rangle$  will be unchanged. The noisy success probability can be obtained by averaging  $P_n(E)$  over the distribution  $p(\delta E_{k,n})$  of the noise:

$$P_{n,\text{noisy}}(E) = \sum_{k} \frac{|\langle E_k | \psi_I \rangle|^2}{2^n} \prod_{i=1}^n \int d(\delta E_{k,i}) p(\delta E_{k,i}) \left[ 1 + e^{-(E_k + \delta E_{k,i} - E)^2 \sigma^2 / 2} \right]. \tag{9}$$

In the simple case where  $\delta E_{k,i}$  is Gaussian distributed with mean 0 and standard deviation  $\varepsilon_k$ , then  $p(\delta E_{k,i}) = \frac{1}{\sqrt{2\pi\varepsilon_k^2}}e^{-(\delta E_k)^2/(2\varepsilon_k^2)}$  and

$$\int d(\delta E_{k,i}) p(\delta E_{k,i}) \left[ 1 + e^{-(E_k + \delta E_{k,i} - E)^2 \sigma^2 / 2} \right] = 1 + \frac{e^{-(E_k - E)^2 \sigma^2 / [2(1 + \varepsilon_k^2 \sigma^2)]}}{\sqrt{1 + \varepsilon_k^2 \sigma^2}} \,. \tag{10}$$

The centers of the peaks thereby remain at  $E_k$ . When the eigenenergies are well-separated, the peak height at  $E=E_k$  is reduced by a factor of  $\left[1+\frac{1}{\sqrt{1+\varepsilon_k^2\sigma^2}}\right]^n/2^n$ , which gives exponential suppression in the number n of cycles. When  $\varepsilon_k^2\sigma_k^2\ll 1$ , one obtains

$$P_{n,\text{noisy}}(E_k) \approx |\langle E_k | \psi_I \rangle|^2 \left[ 1 - \varepsilon_k^2 \sigma^2 / 4 \right]^n$$
 (11)

One can also consider the case when  $\delta E_{k,i} = \delta E_k$  is independent shot-to-shot, but the same for all cycles. This might, for instance, reflect slowly-varying coherent errors arising from calibration inaccuracies. Assuming sufficient sampling that averages over the error distribution,

$$P_{n,\text{noisy}}(E) = \sum_{k} \frac{|\langle E_k | \psi_I \rangle|^2}{2^n} \int d(\delta E_k) p(\delta E_k) \left[ 1 + e^{-(E_k + \delta E_k - E)^2 \sigma^2 / 2} \right]^n . \tag{12}$$

For a Gaussian error distribution, this will again leave the centers of the peaks unchanged. To find the suppression of the peak height, one can set  $E=E_k$  and perform the binomial expansion and the integration. Assuming the peaks are well-separated, one obtains

$$P_{n,\text{noisy}}(E_k) \approx \frac{|\langle E_k | \psi_I \rangle|^2}{2^n} \sum_m \binom{n}{m} \frac{1}{\sqrt{1 + m\varepsilon^2 \sigma^2}} \,.$$
 (13)

Assuming  $m \varepsilon_k^2 \sigma^2 \ll 1$ , then to lowest order one obtains

$$P_{n,\text{noisy}}(E_k) \approx |\langle E_k | \psi_I \rangle|^2 \left[ 1 - n\varepsilon_k^2 \sigma^2 / 4 \right] . \tag{14}$$

In this case, one sees only a linear decay of the peak height in the number of rodeo cycles.